Slow Axonal Transport Mechanisms Move Neurofilaments Relentlessly in Mouse Optic Axons

Raymond J. Lasek,* Paola Paggi,*‡ and Michael J. Katz*§

*Bio-architectonics Center, §Department of Epidemiology and Biostatistics, School of Medicine, Case Western Reserve University, Cleveland, Ohio 44106; and ‡Dipartimento di Biologia Cellulare e dello Sviluppo, Universita' "La Sapienza," 00185 Roma, Italy

Abstract. Pulse-labeling studies of slow axonal transport in many kinds of axons (spinal motor, sensory ganglion, oculomotor, hypoglossal, and olfactory) have led to the inference that axonal transport mechanisms move neurofilaments (NFs) unidirectionally as a single continuous kinetic population with a diversity of individual transport rates. One study in mouse optic axons (Nixon, R. A., and K. B. Logvinenko. 1986. *J. Cell Biol.* 102:647–659) has given rise to the different suggestion that a significant and distinct population of NFs may be entirely stationary within axons. In mouse optic axons, there are relatively few NFs and the NF proteins are more lightly labeled than other slowly transported slow component b (SCb) proteins (which, however, move faster than the NFs); thus, in mouse optic axons, the radiolabel of some of these faster-moving SCb proteins may confuse NF protein analyses that use one dimensional (1-D) SDS-PAGE, which separates proteins by size only. To test this possibility, we used a 2-mm "window" (at 3–5 mm from the posterior of the eye) to compare NF kinetics obtained by 1-D SDS-PAGE and by the higher resolution two-dimensional (2-D) isoelectric focusing/SDS-PAGE, which separates proteins both by their net charge and by their size. We found that 1-D SDS-PAGE is insufficient for definitive NF kinetics in the mouse optic system. By contrast, 2-D SDS-PAGE provides essentially pure NF kinetics, and these indicate that in the NF-poor mouse optic axons, most NFs advance as they do in other, NF-rich axons. In mice, >97% of the radiolabeled NFs were distributed in a unimodal wave that moved at a continuum of rates, between 3.0 and 0.3 mm/d, and <0.1% of the NF population traveled at the very slowest rates of <0.005 mm/d. These results are inconsistent with the proposal (Nixon and Logvinenko, 1986) that 32% of the transported NFs remain within optic axons in an entirely stationary state. As has been found in other axons, the axonal transport system of mouse optic axons moves NFs and other cytoskeletal elements relentlessly from the cell body to the axon tip.

AXONAL transport studies have proved invaluable in making inferences about the as yet invisible microscopic dynamics of many structural elements of cells. In particular, the transported cytoskeletal structures (neurofilaments [NFs],[1] microtubules, and actin microfilaments) are key components of neurons, and their tendency for continual movement is highlighted dramatically in axons (Lasek, 1986, 1988).

Classically, the cytoskeletal dynamics in axons have been studied with pulse-labeling studies (for reviews see Grafstein and Forman, 1980; Brady and Lasek, 1982; Baitinger et al., 1982). Similar axonal transport studies have also provided in vivo physiological information about the natural dynamics of other cellular structures: the membranous elements, the cytomatrix elements (clathrin, spectrin, uncoating ATPase, creatine phosphokinase, and enolase), and the other cytoskeletal elements (actin-microfilaments, microtubules, and neurofilaments) (for reviews see Grafstein and Forman, 1980; Baitinger et al., 1982; Lasek et al., 1984). In all cases, the mechanisms underlying axonal transport of these elements have been found to be active chemo-mechanical motility systems (Schliwa, 1984).

NFs are considered paradigmatic subjects for studies of the axonal transport of cytoskeletal polymers (Lasek and Hoffman, 1976). NFs are specialized polymers which operate as architectural elements, increasing the width, and thereby the conduction velocity of the axon (Lasek et al., 1983; Hoffman et al., 1984, 1988; Lasek, 1988). NF subunits self-assemble into stable polymers, and, once they are assembled, tend to remain assembled (Morris and Lasek, 1982; Black et al., 1986). In the axon, more than 95% of the NF subunits are polymerized stably into NFs (Morris and Lasek, 1982). Because the NF subunits are attached within stable NF polymers in the axon, analyses of the movement of radiolabeled NF protein subunits in the axon represent the movements of fully assembled NF polymers.

1. *Abbreviations used in this paper*: NF, neurofilament; NFH, NF heavy subunit; NFL, NF light subunit; NFM, NF medium subunit; SCa and SCb, slow component a and b of axonal transport; UA, clathrin uncoating ATP-ase.

For many years, our laboratory has used the pulse-labeling method to study slow axonal transport and NF kinetics (e.g., Lasek, 1968; Hoffman and Lasek, 1975; Black and Lasek, 1980; Paggi and Lasek, 1987; Oblinger and Lasek, 1988). From these studies and from those of other laboratories (e.g., Mori et al., 1979; Hoffman et al., 1984, 1985, 1988; Filliatreau et al., 1988; Tashiro and Komiya, 1989), a consistent pattern has emerged: for any set of homogeneous axons, the radio-labeled population of NFs moves undirectionally down axons and is distributed within the axon as a unimodal, smooth, bell-shaped wave. From the accumulated results of these studies, Lasek (1970, 1986, 1988) has suggested that major cytoskeletal proteins are actively and relentlessly transported in the form of polymers that slide past each other as they are moved down the axon.

Individual studies have occasionally been used to suggest other possible cell biological models (Angelides et al., 1989; Bamburg et al., 1986; Lewis and Nixon, 1988; Nixon and Logvinenko, 1986; Stromska and Ochs, 1981; Watson et al., 1990; Lim et al., 1990; Okabe and Hirokawa, 1990). For instance, one often cited study of NF kinetics by Nixon and Logvinenko (1986) puts forth mechanisms that include the laying down or deposition of cytoskeletal proteins into a stationary axonal cytoskeleton. *Science Citation Index* shows that between 1986 (when the Nixon and Logvinenko study was published) and October 1991 the Nixon and Logvinenko paper was cited 46 times. In 33 (72%) of these papers, the citation focused on the possibility of a stationary phase of NFs; moreover, 27 (58%) of the papers used the citation to support a cell biological model or hypothesis (for reviews of stationary cytoskeletal models in axons see Alvarez and Torres, 1985; Bamburg, 1988; Cleveland and Hoffman, 1991; Hollenbeck, 1989; Mitchison and Kirshner, 1988; Ochs, 1982; Nixon, 1987, 1991).

In the Nixon and Logvinenko (1986) study, proteins transported in mouse optic axons were pulse labeled with [^{3}H]proline, and the radiolabeled NF proteins were then analyzed by one dimensional (1-D) SDS-PAGE. From their results, the authors suggest the possibility that there are two kinetically distinct phases or populations of radiolabeled NF proteins within this homogeneous set of axons. Phase I would move at a rate of 0.5–0.7 mm/d. Phase II would be effectively stationary, never reaching the axon terminals during the 2–3 yr lifespan of the mouse optic neurons. Nixon and Logvinenko (1986) suggest that the stationary Phase II includes ~32% of the total NF proteins that are produced by the retinal ganglion cell neurons and then transported into the ganglion cell axons.

One factor that may have contributed to the difference between the results of Nixon and Logvinenko (1986) and those of other studies of NF transport is their particular axonal test system—mouse retinal ganglion cell axons—which have relatively few NFs as compared to many other varieties of axons. The amount of radiolabeled NF subunits is much less in the NF-poor optic axons when compared to the NF-rich oculomotor, spinal motor, and sensory ganglion axons (McQuarrie et al., 1986; Oblinger et al., 1987; Paggi and Lasek, 1987; see also the electron microscopic comparisons of optic axon cross sections in rat optic axons [Monaco et al., 1989] and chicken oculomotor axons [Price et al., 1988, 1990]).

At the same time, in mouse optic axons, other slowly transported proteins, (in particular, the slow component b of the axonal transport [SCb] cytomatrix proteins) are labeled more heavily than the NF proteins and some of these heavily labeled SCb proteins have molecular sizes similar to the NF subunits (Garner and Lasek, 1982; Oblinger et al., 1987). Similar sized SCb proteins are not well separated from the NF subunits by 1-D SDS-PAGE, which distinguishes proteins largely on the basis of their size. In certain axonal test systems with large amounts of transported NF proteins, a small amount of overlap with the SCb proteins may not substantially distort the final results (Lasek and Hoffman, 1976; McQuarrie et al., 1986; Paggi and Lasek, 1987). On the other hand, in those systems (such as the mouse optic system) with only small amounts of NFs, SCb overlap may largely obscure the researcher's view of the individual NF subunits when his sole separation technique is 1-D SDS-PAGE.

These observations suggested that in the mouse optic system 1-D SDS-PAGE alone may be insufficient to separate radiolabeled NF proteins from heavily labeled SCb proteins. Furthermore, the mixture of the faster SCb proteins with the slow moving NFs could make it appear that there are two distinct groups of NF transport rates, a possibility that was suggested by Nixon and Logvinenko (1986). To examine a contrasting possibility, namely that other radiolabeled proteins may contribute to NF kinetics in 1-D SDS-PAGE analyses of the mouse optic system, we studied NF kinetics in mouse optic axons with [^{35}S]methionine and with the higher resolution two-dimensional (2D) isoelectric focusing/SDS-PAGE (2-D SDS-PAGE), which separates proteins both by their net charge and by their size. In the present paper, we detail the kinetics of NFs in the mouse optic system by comparing analyses of proteins separated by 1-D SDS-PAGE and 2-D SDS-PAGE. In brief, we found that the method of 1-D SDS-PAGE alone is insufficient for kinetic studies in those axons (such as the mouse optic system) where the SCa-cytoskeletal and SCb-cytomatrix waves overlap and where the relative proportion of radiolabeled NF proteins is especially low.

Materials and Methods

Isotope Injection and Radiolabeling of Proteins in the Retinal Ganglion Cells

Male C57Bl/6j mice, between six and eight weeks old, were anesthetized with methoxyfluorane (Metofane, Pitman-Moore), and 0.19 mCi of [^{35}S]methionine (specific activity 1,157 Ci/mmol) (New England Nuclear, Boston, MA) or 0.2 mCi of a 1:1 mixture of [^{3}H]leucine and [^{3}H]lysine in 1 μl of saline ([^{3}H]leucine-specific activity 166 Ci/mmol and [^{3}H]lysine-specific activity 85 Ci/mmol) (Amersham Corp., Arlington Heights, IL) was injected into the vitreous humor of the right eye of each mouse as previously described (Paggi et al., 1989). ^{3}H-labeled amino acids were used in experiments which analyzed the longevity of radiolabeled proteins in the mouse optic axons. In these experiments, one of the critical time points was 198 d after the injection, greater than twice the 87-d half-life of ^{35}S.

Dissection of the Nerve Segments for the "Window Method" of Analysis

Mice were anesthetized and then killed by decapitation at 1–170 d after injection. The right optic nerve, the contiguous left optic tract, and the left superior colliculus were dissected from each mouse. For the "window method" of analysis (Paggi et al. 1989), one 2-mm segment of the optic nerve extending from the optic chiasm toward the eye (3–5 mm from the

eye) was collected. An a priori correction (Fisher, 1966) was introduced to deal with the unavoidable variability in the effectiveness of the amount of experimentally introduced [^{35}S]methionine incorporated into the proteins of the retinal ganglion cells of different mice. (For a complete description see Paggi et al., 1989.)

As Brady and Lasek (1982) suggested, the following parameters must be considered when choosing a window for axonal transport experiments: Ideally, the length of the window should be shorter than the length of the transported elements so that a transported element is counted as few times as possible as it passes through the window. As the size of the window increases, the number of times that a transported element is counted during its transit increases, and slower moving transported elements are counted more times than faster moving elements. Because slower moving elements are counted more times than faster moving ones, the slower ones are emphasized in axonal transport kinetics obtained by the window analysis method.

In practice, the physical process of accurately cutting a reproducible segment from the optic nerve physically constrains the length of the window, and the amount of radioactivity in the population of transported elements also limits how short the window segment can be. In pilot experiments, we found that a 2-mm segment provided sufficient radioactivity for accurate 2-D SDS-PAGE data for individual slowly transported protein bands. For comparison, Nixon and Logvinenko (1986) used a 9-mm-long window which was collated from their data for eight consecutive 1.1-mm segments from the entire optic nerve and tract. This 9-mm window tends to emphasize the slower moving elements in the population.

Dissection of the Nerve Segments for Analyses of the Serial Distribution of Radiolabeled Protein in the Optic Axons

For analyses of the distribution of the radiolabeled protein along the full length of the optic axons, the entire right optic nerve and the left optic tract were removed, frozen, and then cut serially into consecutive 1-mm segments using a Mickel gel slicer (Brinkmann Instruments, Inc., Westbury, NY). All segments were used for the analysis.

Analyses of the Amount of the Very Slowest Moving Radiolabeled Proteins in Retinal Ganglion Cells

Mice were injected with a mixture of [^{3}H]leucine and [^{3}H]lysine and killed at 5, 10, 15, 74, and 198 d after the injection. The optic nerves and tracts were removed and cut into consecutive 1-mm segments. To obtain a sufficient amount of radioactivity for 2-D SDS-PAGE analysis at the relatively long intervals of 74 and 198 d, the corresponding 1-mm segments from a number of mice were combined and homogenized in 140 μl of BUST (0.1 M Tris containing 2% beta-mercaptoethanol, 8 M urea, 1% SDS, pH 6.8). In this way, we obtained a consecutive series of nine "pooled" samples representing the optic axons between 0 and 9 mm from the posterior of the eye.

Previously, we (Paggi et al., 1989) have found an unavoidable variability in the amount of radiolabeled amino acids incorporated into the proteins of the retinal ganglion cells of different mice. To deal with this variation, we modified the procedure described in Paggi et al. (1989). In brief, for each postinjection interval, a sample group of 10–20 mice were injected with ^{3}H-amino acids and killed at the appropriate time. Their optic nerves, optic tracts, and superior colliculi were removed, frozen, and stored. The left superior colliculus from each mouse was then analyzed for total radioactive protein, and only those mice were used which achieved 30% of the maximal radiolabeling in the sample group; these were deemed to be effectively labeled. The optic nerve and tract from these animals were cut into consecutive 1-mm segments and the corresponding segments combined. In this way, we obtained nine normalized samples representing consecutive 1-mm segments along the optic pathway from 5–12 effectively labeled mice, which is a sufficient number to produce a fairly uniform experimental "pool" of best case animals (Paggi et al., 1989).

Preparation of the Tissue Extracts

As described elsewhere (Paggi et al., 1989), each segment was homogenized in 250 μl of BUST. The nerve and the tract homogenates were centrifuged at 22,000 *g* (model SS-34; Sorval Instruments, Newton, CT) for 20 min and the superior colliculus (SC) homogenates were centrifuged at ~130,000 *g* (model Ty 65; Beckman Instruments, Inc., Palo Alto, CA) for 1 h (Black and Lasek, 1980). The pellets were discarded, and the supernatants were used to determine total radioactivity and to separate proteins by 1-D SDS-PAGE and 2-D isoelectric focusing/SDS-PAGE.

Electrophoresis and Fluorography

Gradient slab gels (6–17.5% acrylamide) with a 4% stacking gel were used to separate radiolabeled proteins (Paggi et al., 1989) according to the procedure of Laemmli (1970). 2-D isoelectric focusing/SDS-PAGE was performed according to O'Farrel (1975), using the standard range of ampholines, pH 5–7 (LKB Instruments, Inc.,Bromma, Sweden). The molecular mass standards used were (expressed in kD): myosin (205), macroglobulin (180), galactosidase (116), phosphorylase (97), BSA (68), pyruvate kinase (57), ovalbumin (43), carbonic anhydrase (30), and lysozyme (14). The radioactive polypeptides were visualized by fluorography (Paggi et al., 1989) according to the methods of Bonner and Laskey (1974) and Laskey and Mills (1975).

Quantification of Radioactivity in Individual Transported Proteins

Appropriate regions of the 1- and 2-D gels were excised, using the fluorographs to locate the positions of the labeled polypeptides in the gels. Gel slices were then solubilized, and their radioactivity was counted (Paggi et al., 1989). Counts were converted to dpm, correcting them for quenching and isotope decay. For the "window method" of analysis (Paggi et al., 1989), data for individual nerve segments were plotted versus the interval of time between the injection of the radioactive precursor and the collection of the segments for analysis.

For comparison of the transit rates of the transported proteins through the optic axons, we estimated the maximal transit rate for the entry to the nerve window, which was 3 mm from the retina (the posterior surface of the eye), and the minimum transport rate for the exit from the nerve window, which was 5 mm from the retina.

To produce a quantitative summary of the passage of a full population of radiolabeled proteins through the optic nerve window, we estimated the half-transient time, the nearest day at which 50% of the pulse transient has passed through a given window. The pulse transient (Paggi and Lasek, 1987; Paggi et al., 1989) is simply the area under the curve and provides a simple numerical summary of the transport curve through a given axonal window. Such areas were measured with a Sigma Scan digitizer (Jandell Scientific, Corte Madera, California). The half-transient time is a summary of the time that elapses when a population of transported proteins enters, traverses, and exits a window. It is very similar to another summary statistic that we used previously and that we had called the median transit time (e.g., Paggi et al., 1989). (The median transit time is a whole nerve statistic, whereas, the half-transient time is strictly a window statistic. To calculate half transient times from median transit times, subtract the entry time [the time it takes for the first appearance of the protein in the window segment of interest] from the median transit time.)

Results

Slow Transport Waves of the Total Mixture of Radiolabeled Proteins

Fig. 1 illustrates the axonal transport kinetics of radiolabeled slowly transported proteins in the mouse optic system, using the window method of analysis. The segment extending from 3–5 mm from the eye represents a narrow window through which the passage of the transported proteins can be viewed (Paggi and Lasek, 1987; Paggi et al. 1989; and see Materials and Methods). In the window method, the data for the amount of radiolabeled elements are plotted as a function of the time interval between injection of the radioactive precursor and collection of the segments for analysis. Our kinetic transport profiles resemble those reported in other window studies of slowly transported proteins (Grafstein et al., 1972; Nixon and Logvinenko, 1986; Paggi and Lasek, 1987; Paggi et al., 1989). Such window curves have found an asymmetric unimodal wave with a steep rising phase (or front) that crests

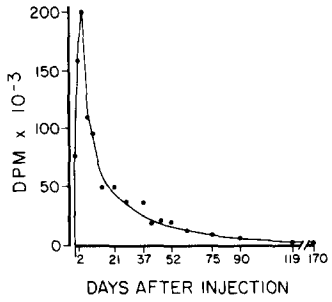

Figure 1. Axonal transport kinetics for the total amount of radiolabeled slowly transported proteins after labeling the retinal ganglion cells with [^{35}S]methionine. Data from a 2-mm optic nerve segment are plotted as a function of the time interval between injecting the radioactive precursor and collecting the segments for analysis. Each data point is the average of 3–11 observations, for a total of 118 observations, from animals killed 1, 2, 4, 7, 10, 15, 21, 28, 37, 42, 47, 52, 61, 75, 90, 119, and 170 d after labeling. The curve is asymmetric, showing a rapid rising phase followed by a gradual declining phase that approached the background level of radioactivity at ~170 d.

in a peak and that finishes with a gradual declining phase gradually approaching background levels at 3–6 mo after labeling.

From the position of the observed maximum at 4 d after labeling, we estimate an overall modal (peak) transit rate of 0.75 mm/d for the slowly transported proteins. This is comparable to the modal transit rate for the slowly transported (SCa and SCb) proteins in optic axons of a variety of rodents (Black and Lasek, 1980; Garner and Lasek, 1982; McQuarrie et al., 1986; Paggi and Lasek, 1989). The declining phase of the curve decreased very rapidly at first and then more slowly until it approached a background level of radioactivity at 120–170 d after the labeling. At 170 d, the amount of slowly transported radioactivity was 1,212 dpm or 0.6% of the peak levels found at 4 d.

1-D SDS-PAGE Analyses

DESCRIPTION OF VISUAL APPEARANCE

To compare the 1-D SDS-PAGE and the 2-D SDS-PAGE analytical methods, we began by documenting the 1-D analyses. Consecutive 1-mm segments of the optic system extending from the back of the eye to the superior colliculus of individual mice were examined by 1-D SDS-PAGE at 7 and 15 d after labeling with [^{35}S]methionine. (At these times, most of the radiolabeled slowly transported proteins are contained within the nerve, the tract, and the terminal regions of the optic axons.) Fig. 2 shows that at 7 d after injection most of the radiolabeled cytomatrix proteins move as a coherent population in axonal segments 5–8, which are located 5–9 mm from the eye. A small amount of the faster moving cytomatrix proteins had already reached the superior collic-

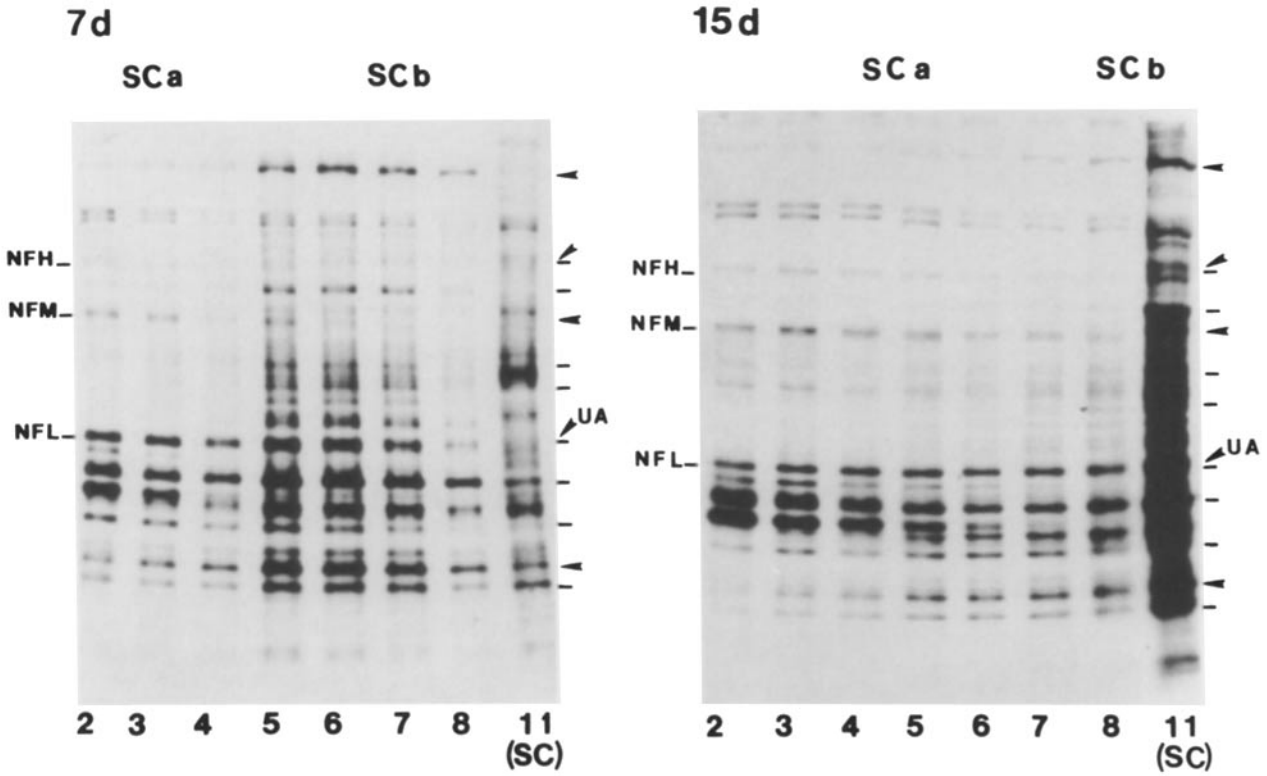

Figure 2. Fluorograph illustrating the distribution of labeled polypeptides in consecutive 1-mm segments of the right optic nerve and left optic tract and in the left superior colliculus (*SC*), 7 and 15 d after injection of [^{35}S]methionine into the vitreous humor of the right eye. The numbers at the bottom of the gel lanes indicate the distance in millimeters from the eye to the proximal end of each segment. Segment 5 (5–6 mm from the eye) corresponds to the chiasm and segment 11 (11–13 mm from the eye) corresponds to the SC. For each segment, the same volume of homogenate was applied to the slab gradient gel (6–17.5% acrylamide). Bars at the right indicate the positions of molecular mass standards (205, 180, 116, 97, 68, 57, 43, and 30 kD reading from top to botton). Arrowheads at the right indicate major polypeptides of the SCb, which is composed of the axonal cytomatrix proteins. Other labels indicate the bands corresponding to the gel kD regions where the 70-kD UA and the neurofilament proteins (NFL, NFM, and NFH) are located. The positions of the NF and the SCb-cytomatrix waves are noted above each gel.

ulus(~11 mm from the eye), and a trail of slower moving cytomatrix proteins was still present in axonal segments 2–5, which are located 2–6 mm from the eye. (The distribution of the cytomatrix proteins is especially distinct for five proteins of >300, 180, 145, 70, and 30–35 kD, as indicated by arrow heads in Fig. 2.)

At 7 d after injection, the three NF triplet protein subunits (NF light protein [NFL], medium protein [NFM], and heavy protein [NFH]) and other SCa proteins are present in the proximal part of the optic axons 2–6 mm from the eye (segments 2–5 in Fig. 2). At this time, the distributions of radiolabeled NFs and certain SCb cytomatrix proteins overlap. For example, the distribution of NFL, the smallest of the triplet NF proteins, overlaps with a faster moving cytomatrix protein, the 70-kD uncoating ATPase (UA) (deWaegh and Brady, 1989; Black et al., 1991), which has approximately the same molecular weight as NFL.

By 15 d after injection, most of the cytomatrix proteins had reached the superior colliculus. Nonetheless, some cytomatrix proteins move more slowly and these form a trail that overlaps the SCa wave. For example, at this time point some of the radiolabeled 30–35-kD cytomatrix proteins are still present in the axons between 3 and 9 mm (segments 3–8 in Fig. 2), where they overlap the slower moving population of SCa-cytoskeletal proteins, which are distributed broadly between 2 and 9 mm from the eye (segments 2–8 in Fig. 2).

The relatively heavy labeling of the cytomatrix proteins, the lighter labeling of the NF proteins (especially NFH), and the overlap between trailing parts of the cytomatrix protein population and the front of the NF protein population, all produce uncertainty as to the exact distribution of the NF proteins in these radiolabeling experiments. For example, even careful examinations of 1-D SDS-PAGE fluorographs (like those in Fig. 2) cannot distinguish the tail of the heavily labeled UA protein wave from the front of the NFL wave. Only NFM is both sufficiently radioactive and clearly separate from other cytomatrix proteins to be distinguished in 1-D gels. Even in this case, however, the background composed of other labeled cytomatrix proteins may confuse 1-D SDS-PAGE analyses of NFM kinetics in mouse optic axons.

QUANTIFICATION OF RADIOACTIVITY IN 1-D SDS-PAGE PROTEIN BANDS

To graph the distributions of the slowly transported proteins on 1-D SDS-PAGE, the amount of radioactivity in the bands at 70 kD (a region containing both NFL and UA) and at 145 kD (a region containing NFM) was quantified. Fig. 3 *A* shows the transport profiles for these bands in the optic nerve window. The waveforms of the 70- and 145-kD bands were similar to those of the total mix of slowly transported proteins shown in Fig. 1. Like the total proteins, the observed maxima of the 70- and the 145-kD bands occurred at 4 d in the optic nerve window and the initial rapidly declining phase of the curves was followed by a broader phase that declined more slowly.

The described waveforms and their similarity to the curves for the kinetics of transport for the whole mixture of slowly transported proteins (Fig. 1) suggest that in 1-D SDS-PAGE separations of slowly transported proteins in the mouse optic system the 70- and 145-kD gel regions contain a mixture of faster moving SCb-cytomatrix proteins and slow moving SCa proteins. In particular, the waveform of the 70-kD protein accords with the visual impression of the 1-D SDS-PAGE fluorographs (Fig. 2) that the cytomatrix protein, UA, dominates this particular molecular weight range and overshadows the much smaller amount of like-sized radiolabeled NF protein, namely the NFL protein.

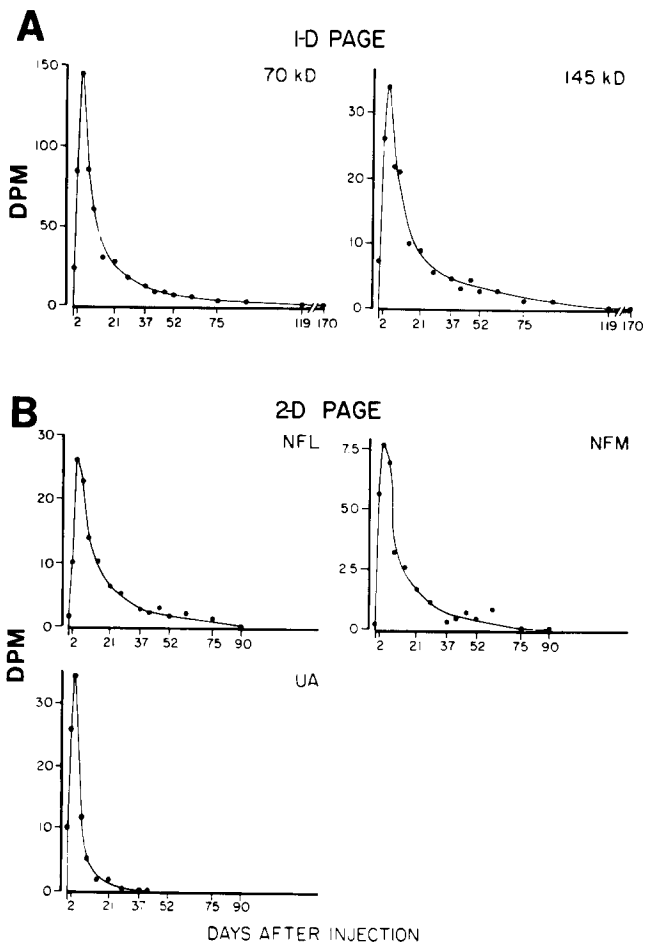

Figure 3. Axonal transport kinetics of radiolabeled (*A*) 70- and 145-kD proteins and (*B*) 70-kD UA and neurofilament proteins (*NFL* and *NFM*) after labeling the retinal ganglion cells with [^{35}S]methionine. (*A*) Fluorographs of 1-D polyacrylamide gels (like those in Fig. 2) were used to remove the gel regions containing the 70- and 145-kD proteins. Data for a 2-mm segment of the optic nerve are plotted as a function of the time interval between injecting the radioactive precursor and collecting the segments for analysis. Each data point is the average of 3–11 observations for a total of 118 observations from animals killed at 1, 2, 4, 7, 10, 15, 21, 28, 37, 42, 47, 52, 61, 75, 90, 119, and 170 d after labeling. The shape of each of the curves is similar to that seen for the total slowly transported proteins in Fig. 1. (*B*) Fluorographs of 2-D SDS-PAGE (like those in Fig. 4) were used to remove the gel regions containing the UA, NFL, and NFM proteins. Data were obtained and plotted as described above and in Materials and Methods. Each data point is the average of 3–11 observations for a total of 109 observations from animals killed at 1, 2, 4, 7, 10, 15, 21, 28, 37, 42, 47, 52, 61, 75, and 90 d after labeling. Overall, the UA curve shape is similar to that of the curves in *A*; however, it lacks the slower and extended declining phase of the curve. The NFM and NFL curves show a rising phase that is slower than the UA curve and a very broad declining phase that is similar to the curves in *A*.

2-D SDS-PAGE Analyses

DESCRIPTION OF VISUAL APPEARANCE

Fig. 4 shows representative 2-D SDS-PAGE fluorographs of the slowly transported proteins in the mouse optic nerve window at 4, 7, and 21 d after labeling. At 4 d, when the crest of the SCb-cytomatrix and SCa protein waves is present in the optic nerve (Fig. 3 *A*), the UA spot is as intense as the NFL spot. At 7 d, when both the SCb-cytomatrix proteins and the SCa proteins begin to decline, the NFL spot is more intense than the UA spot. At 21 d, the intensity of the SCb-cytomatrix proteins and the NF proteins have declined notably.

Fig. 4 shows that the 2-D SDS-PAGE method clearly separates NFL from UA, and these fluorographs confirm that at least two proteins (UA and NFL) contribute to the radioactivity in the 1-D SDS-PAGE band at the 70-kD location. In addition, there may be other SCb proteins with this molecular size that have isoelectric points outside the range of our isoelectrophoretic focusing procedure, although present in our 1-D SDS-PAGE gels, these proteins would be lost from our particular 2-D SDS-PAGE analyses.

QUANTIFICATION OF RADIOACTIVITY IN SPECIFIC 2-D SDS-PAGE PROTEIN SPOTS

To determine the transport kinetics of the slowly transported proteins separated by 2-D SDS-PAGE, three specific proteins—UA, NFL, and NFM—were excised from 2 D SDS-PAGE of the nerve window at many time points between 1 and 90 d after labeling. Fig. 3 compares these 2-D SDS-PAGE transport profiles (Fig. 3 *B*) with the 1-D SDS-PAGE transport profiles (Fig. 3 *A*).

Cytomatrix 70-kD UA. The specific UA waveform from 2-D gels (Fig. 3 *B*) is much sharper than the wave of total radioactivity (Fig. 1) and it is also sharper than the total 70-kD band excised from 1-D gels (Fig. 3 *A*). In the optic nerve window, labeled UA first appeared <24 h after labeling. The radioactive wave then rose quickly, and after reaching a maximum, it declined almost as sharply with only a small trailing edge that approached background levels by 37 d.

The sharp rise and fall of the UA waveform with its single peak are consistent with a single population of proteins moving exclusively with the cytomatrix complex of a homogeneous set of axons. From the positions of the front, the peak, and the tail in the optic nerve window (3–5 mm from the eye), we estimate that the fastest UA proteins are transported at a rate of >3 mm/d and that the slowest proteins move at 0.1 mm or less per day (but fully clearing the window at 37 d after injection).

Neurofilament Proteins: NFL and NFM. Fig. 3 *B* shows that the waveforms of the two NF subunits, NFL and NFM, were similar. In the optic nerve, both the NFL and the NFM waves rose sharply after a significant delay. (For example, at 1 d after labeling a small amount of radiolabeled NF protein had reached the optic nerve window, while at 4 d the NFL and NFM waveforms were unimodal and peaked sharply.)

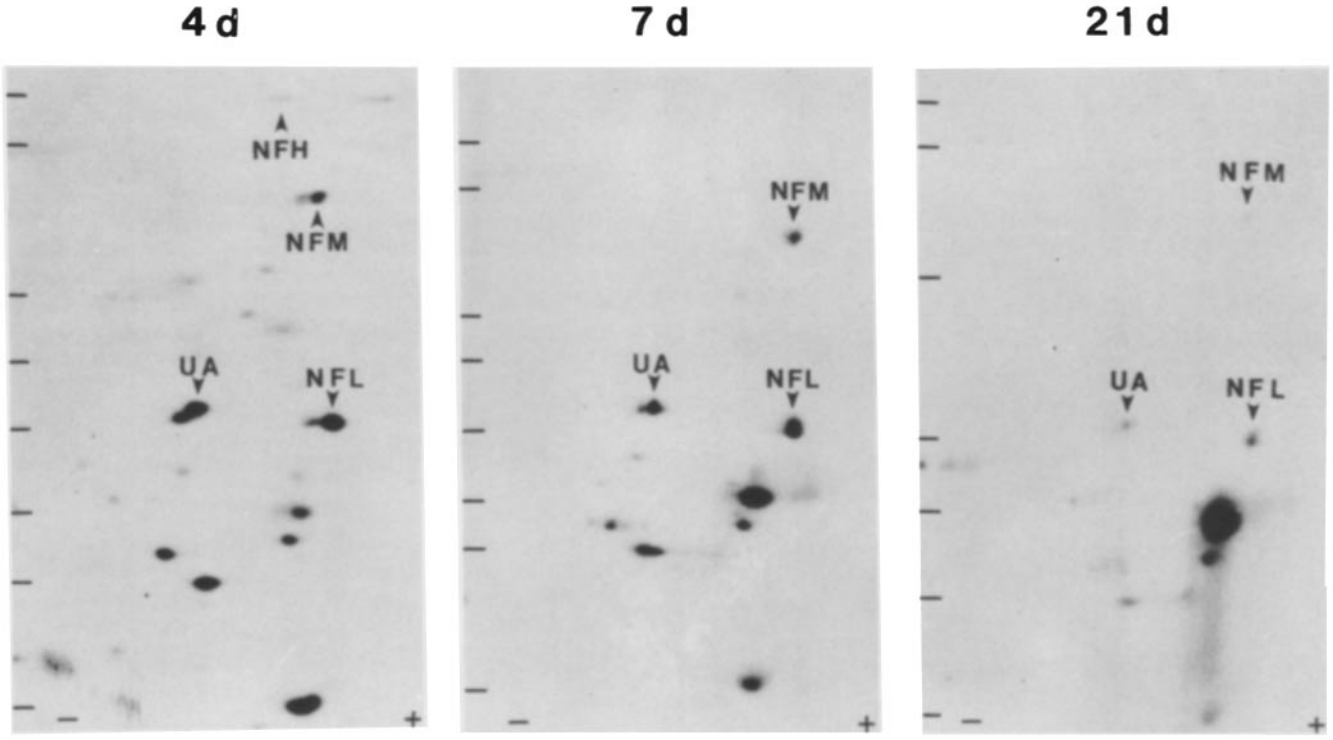

Figure 4. Fluorographs showing labeled polypeptides separated by 2-D SDS-PAGE at 4, 7, and 21 d after labeling the retinal ganglion cells with [^{35}S]methionine. Aliquots of homogenates of the optic nerve segments were subjected to isoelectric focusing in the first dimension; then they were analyzed on 6–17.5% gradient slab polyacrylamide gels in the second dimension. The acidic and basic ends of the gels are indicated in the figure. Bars along the left show the positions of the molecular mass standards (200, 180, 116, 97, 68, 57, 43, and 30 kD reading from top to bottom). The spots corresponding to the neurofilament proteins (*NFH*, *NFM*, *NFL*) and to the 70-kD UA are labeled.

Then the waveforms descended slowly in a gradual and long trail that approached background levels at 90 d.

From the front of the labeled NFL wave in the optic nerve window, we estimate a maximum transport rate of more than 3 mm/d. From the tail of the waveform, we estimate that some NFs move with an effective rate of <0.03 mm/d.

Comparisons of NFL, UA, and 70 kD. To compare the waveforms of NFL and UA from the 2-D SDS-PAGE analyses with the 70-kD band from the 1-D SDS-PAGE analyses, we normalized each set of radiolabeled proteins by considering the maximum observed radioactivity in the optic nerve window as 100%. The normalized results for the period from 1 to 7 d are plotted in Fig. 5. From 1 to 4 d after labeling, the UA waveform rose most rapidly, the NFL waveform rose most slowly, and the 70-kD band waveform was intermediate between UA and NFL, Similarly, from 4 to 7 d, the UA waveform descended most rapidly, the NFL waveform descended most slowly, and the 70-kD waveform was intermediate between UA and NFL.

To further compare the passage of the radiolabeled proteins through the optic nerve window, we estimated the half-transient time (the time that it takes for 50% of a radiolabeled population to traverse a window) (see Materials and Methods and also Paggi et al., 1989 for details). The half-transient times for NFL, the 70-kD band, and UA were 13, 10, and 4 d, respectively. As with the fuller graphic comparison of the transport distributions in Fig. 5, the half-transient time of the 70-kD band was intermediate between those of NFL and UA. These results are consistent with the proposal that the transport kinetics of the 70-kD band as analyzed on 1-D SDS-PAGE combines a mixture of SCb proteins (principally UA proteins) and the more slowly transported NFL proteins.

Quantification of the Very Slowest Moving NF Proteins. The shapes of the NFL and the NFM waves in Fig. 3 *B* suggest that nearly all the axonally transported NF proteins had entered and exited the optic nerve window by 90 d after labeling. More specifically, quantitative comparison of the NFs remaining in the nerve window after the main population of NFs have cleared, it shows that <3% of the peak amount of NFs (those which are in transit at 4 d moving at 0.75 mm/d) remain in transit at 90 d (moving at 0.03 mm/d).

To determine unequivocally the amount of axonally transported NFs that move very slowly in the optic axons, mice were injected with [^{3}H]leucine and [^{3}H]lysine, then killed 5, 10, 15, 74, and 198 d later. Fig. 6 *A* shows the serial distributions of the NFL, NFM, and NFH subunits in optic axons obtained by 2-D SDS-PAGE at 10 d after injection, a time when the maximum population of radiolabeled NF is present in the optic nerve and tract. This can be compared with Figs. 6, *B* and *C*, which show the distributions at 74 and 198 d after injection, a time when most of the NFs have cleared the optic axons.

At 10 d after injection, the peak of the wave of radiolabeled NF is between segments 3 and 4 (2–3 and 3–4 mm from the

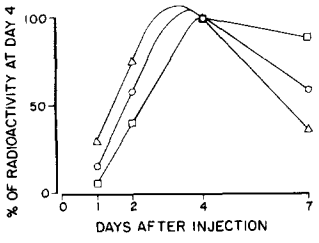

Figure 5. Axonal transport kinetics of radiolabeled 70-kD protein (○), 70-kD UA (△), and neurofilament protein, NFL (□) after labeling the retinal ganglion cells. Here, the data presented in Fig. 3 are expressed for each protein as a percentage of the respective radioactivity that each protein presented in the nerve segment at 4 d after the labeling injection. The slopes of both the rising and the declining phases of 70-kD kinetics curve are intermediate between those of the UA and the NFL curves.

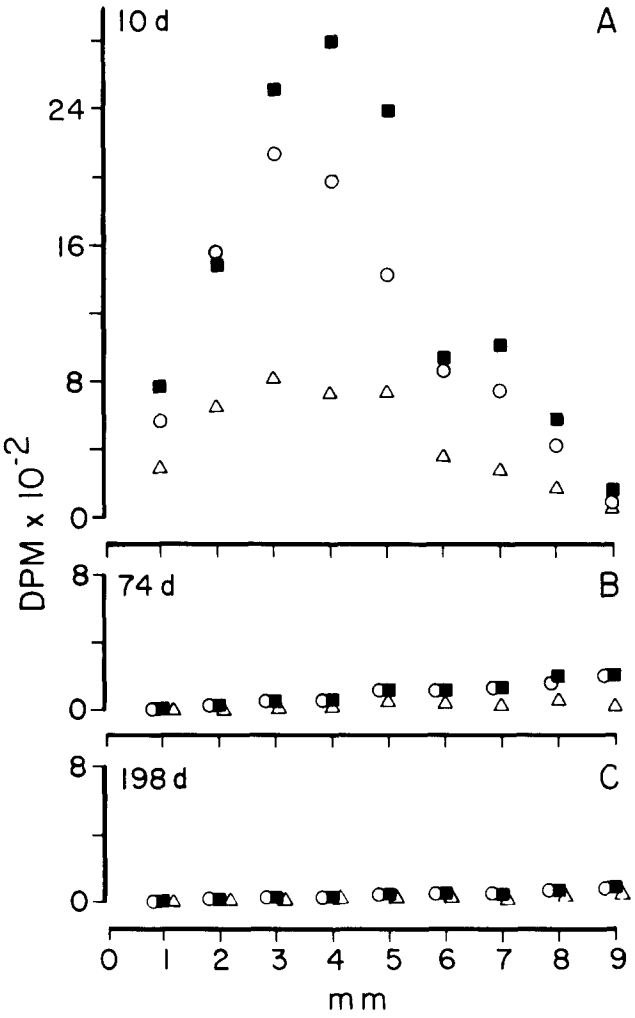

Figure 6. Axonal transport kinetics of radiolabeled neurofilament proteins (NFL, ■; NFM, ○; NFH, △) after labeling the retinal ganglion cells with [^{3}H]leucine and [^{3}H]lysine. Fluorographs of 2-D SDS-PAGE (like those in Fig. 4) were used to remove the gel regions containing NFL, NFM, and NFH proteins. Data for consecutive 1-mm segments of the entire optic nerve and tract are plotted as a function of the distance in millimeters from the eye to the distal end of each segment. Each data point is an average of 5, 6, or 12 mice for 10 (*A*), 74 (*B*), or 198 (*C*) days, respectively. The average was obtained by combining the corresponding 1-mm segments from a number of mice into one sample and a constant-sized aliquot was then analyzed by 2-D SDS-PAGE. The amount of radiolabeled NF proteins decreases markedly between 10 and 74 d after labeling and continues to decrease between 74 and 198 d after labeling.

eye). At that time, most of the radiolabeled NF subunits are contained within the optic pathway (Fig. 6 *A*). By contrast, at 74 d after injection (Fig. 6 *B*), only the trailing part of the population of radiolabeled subunits remain in the optic axons and these residual proteins are distributed in a declining tail that decreased gradually from segment 9 to segment 1. The amount of radiolabeled NF declined further between 74 and 198 d after injection, and the slope of the distribution at 198 d was flatter than at 74 d, suggesting that the tail of radiolabeled NF proteins declines continually after the main wave has traversed the axons (Fig. 3 *B*). It appears that NF subunits are cleared continually from the optic axons, as would be consistent with mechanisms of slow axonal transport operating continually to move all of the NFs toward the axon terminals.

In our study, the slowest moving NFs are present in segment 1 at 198 d after injection. Traveling at an overall rate of <0.005 mm/d, these NF subunits contained 17, 19, and 0 dpm for NFL, NFM, and NFH, respectively. A comparison of these amounts of very slow moving radiolabeled NF with the amount in the peak of the radiolabeled NF population (segments 3 or 4 at 10 d after injection in Fig. 6 *A*) indicates that <0.9% of the NF proteins travel at the very slowest rates. Undoubtedly, this overestimates the actual amount of very slow-moving NF proteins, those lagging well behind the bulk of the radiolabeled NF. For example, from the sum of the radiolabeled NFL protein at 10 d after injection (when the bulk of the wave of radiolabeled NFL subunits are present in segments 1–9 [Fig. 6 *A*]), almost 13,000 dpm of radiolabeled NFL proteins had traversed segment 1 (with the bulk population moving at rates >0.1 mm/d), whereas only 17 dpm or 0.1% of the total NFL traversed segment 1 at rates <0.005 mm/d.

The declining slopes of the curves at the later postinjection intervals (45–90 d in Fig. 3 *B*, 74 d in Fig. 6 *B*, and 198 d in Fig. 6 *C*) show that even the slowest of the radiolabeled NF proteins continue to move down the optic axons toward the axon terminals. Taken together, these results suggest that if there are any entirely "stationary" NFs in mouse optic axons, as Nixon and Logvinenko (1986) have suggested, their number is exceedingly small by comparison to the moving population of NFs, which traverses the mouse optic axons at rates between 0.05 and 3 mm/d.

Discussion

2-D SDS-PAGE Effectively Separates the Lightly Radiolabeled NF Proteins from Other Heavily Labeled Proteins

We studied the passage of radiolabeled slowly transported proteins through a segment (window) of mouse optic axons. Our results indicate that a mix of slowly transported proteins (principally SCb cytometric proteins) with similar molecular weight contributes to the radiolabeled proteins associated with [^{35}S]methionine-labeled NFL and NFM bands on 1-D SDS-PAGE patterns from mouse optic axons. At the same time, we found that 2-D SDS-PAGE effectively separated the NF protein subunits from other heavily labeled cytomatrix proteins.

Comparisons of the kinetics of NF subunits in mouse optic axons by 1-D SDS-PAGE and 2-D SDS-PAGE show that the lightly radiolabeled NF proteins are mixed together with faster moving SCb-cytomatrix proteins that have molecular weights similar to the NF proteins. In this particular axonal system, the SCb-cytomatrix proteins dominate the transport profiles and the NFL band coincides with a cytomatrix protein, UA, which can easily be distinguished on 2-D gels. We could not distinguish any specific cytomatrix proteins with molecular weights similar to NFM. However, the kinetic patterns and the much larger amount of radioactivity in the 145-kD 1-D SDS-PAGE band (Fig. 3) as compared with the more purified NFM 2-D SDS-PAGE spot indicate that this protein is also intermixed with cytomatrix proteins on 1-D SDS-PAGE. Likewise, Willard (1977) and Lewis and Nixon (1988) have shown that there are a number of distinct 200-kD cytomatrix proteins that produce a mixture of radiolabeled cytomatrix and NFH protein subunits on 1-D SDS-PAGE. A large number (perhaps hundreds) of radiolabeled proteins with various molecular sizes compose the axonally transported cytomatrix and this multitude of proteins merges together on 1-D SDS-PAGE to produce an overall background gray level of unresolved radiolabeled proteins (Brady et al., 1981; Brady and Lasek, 1981; Garner and Lasek, 1982; Lasek et al., 1984).

Figs. 2–4 show that in the mouse optic system there is a heavy radiolabeling of the slowly transported SCb-cytomatrix proteins. At least two different SCb proteins, each with a different transport rate, contribute to the 1-D SDS-PAGE band in the NF protein region. The labeled SCb proteins complicate interpretations of the 1-D SDS-PAGE fluorographs in the regions of the NF proteins and have contributed to an inappropriate inference (Nixon and Logvinenko, 1986) that there may be two distinct kinetic populations of NFs in optic axons, one population that is moving and another that is entirely stationary.

NF Kinetics in Mouse Optic Axons Resemble Those in Other Axons

Like the other axonal transport studies of rodent optic systems (and like the studies in other populations of axons) (Hoffman and Lasek, 1975; Black, 1978; Mori et al., 1979; Hoffman et al., 1985; McQuarrie et al., 1986; Oblinger et al., 1987; Paggi and Lasek, 1987; Oblinger and Lasek, 1988; Garner, 1988), our present kinetic studies in the mouse indicate that: (*a*) Nfs can be detected moving at a wide range of rates; (*b*) most NFs move at a single modal (peak) rate; (*c*) within the range of rates, the fewest NFs move at the extremely fast or extremely slow rates and an increasing number of NFs move at rates approaching the mode from either extreme.

Studies of many different kinds of axons have found that the peak or modal transport rate in the NF population ranges between 0.1 and 2.0 mm/d. Axons that differ either phylogenetically, ontogenetically, structurally, or metabolically also differ in their modal transport rates. For example, in mammals, modal transport rates are 0.1–0.75 mm/d in optic axons, 0.5–0.1 mm/d in central axons of sensory ganglion cells, 1.0–1.5 mm/d in peripheral axons of sensory ganglion cells, and 1–1.5 mm/d in spinal motor axons (Oblinger et al., 1987; Oblinger and Lasek, 1988). The fastest observed peak rate is 3.6 mm/d for developing spinal motor axons (Hoffman et al., 1985), and the slowest observed peak rate is 0.02 mm/d

for goldfish optic axons (McQuarrie, 1984). In general, optic axons have relatively slow peak NF rates: in mice, rats, and guinea pigs these rates are 0.20–0.75 mm/d (Black and Lasek, 1980; Nixon and Logvinenko, 1986; Oblinger et al., 1987). Some test systems show kinetic curves with more than one mode, and in such experimental paradigms, it has always been found that the axonal population being studied is, in fact, distinctly heterogeneous. For example, Paggi and Lasek (1987) described two modal rates in the oculomotor axons of the chicken, with peak transport rates of 0.26 and 0.73 mm/d. There, the test system could be subdivided into two different populations of axons. The oculomotor population contained structurally, metabolically, and ontogenetically different axons, namely, the parasympathetic oculomotor axons and the somatic motor axons (Price et al., 1988).

In All Axons, NF Kinetics Indicate That the Slow Axonal Transport Mechanisms Move NFs Relentlessly to the Terminals

Usually, kinetic studies of NFs focus on a single average measure, such as the peak (the median) of the transported wave. However, the full NF transport curves embody a diverse set of individual NF rates (Mori et al., 1979; Paggi and Lasek, 1987). For example, we have found that the NF transport rates in mouse optic axons range from >3.0 to <0.03 mm/d, with a median transport rate of 0.2 mm/d. The smooth contour of the full NF transport curve suggests that the diversity of rates within the actual population of NFs forms a continuum that our present methods do not resolve, with NFs moving at fast, slow, and intermediate rates. Paggi et al. (1989) have noted that a heterogeneity of transport rates is characteristic of all axonally transported elements, including the membranous elements of the fast component (Gross and Beidler, 1975), the SCb cytomatrix elements, and the SCa cytoskeletal elements (Cancalon, 1979; Paggi et al., 1989).

In long axons with relatively large numbers of NFs, such as the hypoglossal, the spinal motor, and the spinal ganglion cell axons of rats and guinea pigs, the full population of radiolabeled proteins can be captured in the axons at one time point. The full heterogeneity and variety of NF rates can be contrasted directly in such systems. Even in these systems, there is no evidence of a permanently stationary phase. The NF transport profile (plotted as dpm per unit length of axon) at 1 and 2 mo after labeling is symmetric and there is no substantial "tail" on the curves (Hoffman and Lasek, 1975; Lasek and Hoffman, 1976; Black, 1978; Mori et al., 1979; Lasek et al., 1983; Hoffman et al., 1984, 1985; Oblinger et al., 1987; Paggi and Lasek, 1987; Oblinger and Lasek, 1988).

In the mouse optic system, a small number of NFs advance very slowly, at transit rates as low as 0.005 mm/d. However, even in the mouse, >97% of the NF proteins have entered and passed through the optic nerve within 3 mo (Fig. 3 *B*), and >99.9% have traversed the proximal part of the optic axons within 7 mo (Fig. 6 *C*). Likewise, in experiments with even longer postlabeling intervals, Garner (1988) found that in the guinea pig visual system >99% of the NFs cleared the optic axons within 8 mo of their synthesis. These results are inconsistent with a proposal (Nixon and Logvinenko, 1986) that one third of the NFs remain within rodent optic axons in an entirely stationary state.

Transport studies of the neurofilament system are somewhat simpler than transport studies of other axonal polymer systems. This is because only a very small amount of neurofilament protein is found as monomer within the axon (Morris and Lasek, 1984). Other dynamic molecular aggregates within axons, such as the microtubule systems and the microfilament systems, contain much larger amounts of monomeric protein. In axons, both tubulin and actin apparently exchange between the nondiffusible actively transported polymeric state and the diffusible monomeric state (for review see Lasek, 1988). In the present study, we have focussed on the neurofilament system; nonetheless, we did obtain information about the kinetics of other axonal proteins. As with the neurofilaments, we found that >99% of both the actin and the tubulin cleared the optic axons within seven months of their synthesis; specifically, >99.9% of the actin had cleared the axon by 119 d and >99% of the tubulin had cleared the axon by 170 d.

Unlike the neurofilament proteins, axonal actin and tubulin can spend much of their time in the monomeric state. During that time, these molecules move freely in response to thermal forces. The randomizing effects of Brownian motion move small molecules in many directions, and these molecules can go retrograde, anterograde, or radially. This thermal motion delays the anterograde transport of the labelled polymers, as portrayed in our transport studies. Nonetheless, typical axonal kinetic studies show that anterograde slow transport mechanisms clear the axon proper of actin and tubulin (Paggi and Lasek, 1987). For instance, axonal actin spends 40–50% of its time in the diffusible monomeric state (Morris and Lasek, 1984); yet the slow transport mechanisms actively clear actin from the axon more quickly than they clear the neurofilaments.

NFs are among the slowest moving structures in axons, and their rate of translocation decreases in old age (McQuarrie et al., 1989). Nevertheless, like other faster moving cytoskeletal and membranous elements in the axon, NFs respond to the active dynamics of axonal transport mechanisms. These mechanisms give axons their vitality, relentlessly moving the NFs and other subcellular elements from the cell body to the axon tip during the entire lifetime of the animal.

We thank Shirley Ricketts and Diane Kofskey for providing excellent technical assistance.

This research was supported by awards from the National Institutes of Health to R. J. Lasek and M. J. Katz.

Received for publication 7 November 1991 and in revised form 28 January 1992.

References

Alvarez, J., and J. C. Torres. 1985. Slow axonal transport: a fiction? *J. Theor. Biol.* 112:627–651.

Angelides, K. J., K. E. Smith, and M. Takeda. 1989. Assembly and exchange of intermediate filament proteins of neurons: neurofilaments are dynamic structures. *J. Cell Biol.* 108:1495–1506.

Baitinger, C., J. Levine, T. Lorenz, C. Simon, P. Skene, and M. Willard. 1982. *In* Axonal Transport. D. Weiss, editor. Springer-Verlag New York Inc., New York. 110–120.

Bamburg, J. R. 1988. The axonal cytoskeleton: stationary or moving matrix? *TINS (Trends Neurosci.)* 11:248–249.

Bamburg, J. R., D. Bray, and K. Chapman. 1986. Assembly of microtubules at tips of growing axons. *Nature (Lond.).* 321:788–790.

Black, M. M. 1978. Axonal transport of cytoskeletal proteins. Ph.D. thesis. Case Western Reserve University. Cleveland, Ohio. 97 pp.

Black, M. M., and R. J. Lasek. 1980. Slow components of axonal transport: two cytoskeletal networks. *J. Cell Biol.* 86:616–623.

Black, M. M., P. Keyser, and E. Sobel. 1986. Interval between the synthesis and assembly of cytoskeletal proteins in cultured neurons. *J. Neurosci.* 6:1004–1012.

Black, M. M., M. H. Chestnut, T. Pleasure, and J. H. Keen. 1991. Stable clathrin: uncoating protein (hsc 70) complexes in intact neurons and their axonal transport. *J. Neurosci.* 11:1163–1172.

Bonner, W. M., and R. A. Laskey. 1974. A film detection method for tritium labelled proteins and nucleic acids in polyacrylamide gels. *Eur. J. Biochem.* 46:83–88.

Brady, S. T., and R. J. Lasek. 1981. Nerve-specific enolase and creatine phosphokinase in axonal transport: soluble proteins and the axoplasmic matrix. *Cell.* 23:515–523.

Brady, S. T., and R. J. Lasek. 1982. Axonal transport: a cell-biological method for studying proteins that associate with the cytoskeleton. *Methods Cell Biol.* 25:365–398.

Brady, S. T., M. Tytell, K. Heriot, and R. J. Lasek. 1981. Axonal transport of calmodulin: a physiological approach to identification of long-term association between proteins. *J. Cell Biol.* 89:607–614.

Cancalon, P. 1979. Influence of temperature on the velocity and on the isotope profile of slowly transported proteins. *J. Neurochem.* 32:997–1007.

Cleveland, D. W., and P. N. Hoffman. 1991. Slow axonal transport models come full circle: evidence that microtubule sliding mediates axon elongation and tubulin transport. *Cell.* 67:453–456.

de Waegh, S., and S. T. Brady. 1989. Axonal transport of clathrin uncoating ATPase (HSC70): a role for HSC70 in the modulation of coated vesicle assembly in vivo. *J. Neurosci. Res.* 23:433–440.

Filliatreau, G., P. Denoulet, B. de Nechaud, and L. Di Giamberardino. 1988. Stable and metastable cytoskeletal polymers carried by slow axonal transport. *J. Neurosci.* 8:2227–2233.

Fisher, R. A. 1966. The Design of Experiments. 8th ed. Haffner Publishing Co., Inc., New York. Chapter IX, Section 56: 168–171.

Garner, J. A. 1988. Differential turnover of tubulin and neurofilament proteins in central nervous system neuron terminals. *Brain Res.* 458:309–318.

Garner, J. A., and R. J. Lasek. 1982. Cohesive axonal transport of the slow component b complex of polypeptides. *J. Neurosci.* 2:1824–1835.

Grafstein, B., and D. S. Forman. 1980. Intracellular transport in neuron. *Physiol. Rev.* 60:1197–1283.

Grafstein, B., M. Murray, and N. A. Ingoglia. 1972. Protein synthesis and axonal transport in retinal ganglion cells of mice lacking visual receptor. *Brain Res.* 44:37–48.

Gross, G. W., and L. M. Beidler. 1975. A quantitative analysis of isotope concentration profiles and rapid transport velocities in the C-fibres of the garfish olfactory nerve. *J. Neurobiol.* 6:213–232.

Hoffman, P. N., and R. J. Lasek. 1975. The slow component of axonal transport. Identification of major structural polypeptides of the axon and their generality among mammalian neurons. *J. Cell Biol.* 66:351–366.

Hoffman, P. N., J. W. Griffin, and D. L. Price. 1984. Control of axonal caliber by neurofilament transport. *J. Cell Biol.* 66:351–366.

Hoffman, P. N., J. W. Griffin, B. G. Gold, and D. L. Price. 1985. Slowing of neurofilament transport and the radial growth of developing nerve fibers. *J. Neurosci.* 5:2920–2929.

Hoffman, P. N., E. H. Koo, N. A. Muma, J. W. Griffin, and D. L. Price. 1988. Role of neurofilaments in the control of axonal caliber in myelinated nerve fibers. *In* Intrinsic Determinants of Neuronal Form and Function. R. J. Lasek and M. M. Black, editors. *Neurology and Neurobiology.* Alan R. Liss Inc., New York. 37:389–402.

Hollenbeck, P. J. 1989. The transport and assembly of the axonal cytoskeleton. *J. Cell Biol.* 108:223–227.

Laemmli, V. K. 1970. Cleavage of structural proteins during the assembly of the head of bacteriophage T4. *Nature (Lond.).* 227:680–685.

Lasek, R. J. 1968. Axoplasmic transport in cat dorsal root ganglion cells: as studied with 3H-1-leucine. *Brain Res.* 7:360–377.

Lasek, R. J. 1970. Protein transport in neurons. *Int. Rev. Neurobiol.* 13:289–324.

Lasek, R. J. 1986. Polymer sliding in axons. *J. Cell Sci. Suppl.* 5:161–179.

Lasek, R. J. 1988. Studying the intrinsic determinants of neuronal form and function. *In* Intrinsic determinants of neuronal form and function. R. J. Lasek and M. M. Black, editors. *Neurology and Neurobiology.* Alan R. Liss Inc., New York. 37:3–58.

Lasek, R. J., and P. N. Hoffman. 1976. The neuronal cytoskeleton, axonal transport and axonal growth. *Cold Spring Harbor Conf. Cell Proliferation.* 3:1021–1049.

Lasek, R. J., I. G. McQuarrie, and S. T. Brady. 1983. Transport of cytoskeletal and soluble proteins in neurons. *In* Biological Structures and Coupled Flows. A. Opiatka and M. Balaban, editors. Academic Press Inc., New York and Balaban ISS, Philadelphia. 329–347.

Lasek, R. J., M. M. Oblinger, and P. F. Drake. 1983. Molecular biology of neuronal geometry: expression of neurofilament genes influences axonal diameter. *CSH Symp. Quant. Biol.* XLVIII:731–744.

Lasek, R. J., J. A. Garner, and S. T. Brady. 1984. Axonal transport of the cytomatrix. *J. Cell Biol.* 99:212s–221s.

Laskey, R. J., and A. D. Mills. 1975. Quantitative film detection of ^{3}H and ^{14}C in polyacrylamide gels fluorography. *Eur. J. Biochem.* 56:335–341.

Lewis, S. E., and R. A. Nixon. 1988. Multiple phosphorylated variants of the high molecular mass subunit of neurofilaments in axons of the retinal cell neurons: characterization and evidence for their differential association with stationary and moving neurofilaments. *J. Cell Biol.* 107:2689–2701.

Lim, S. S., K. J. Edson, P. C. Letourneau, and G. G. Borisy. 1990. A test of microtubule translocation during neurite elongation. *J. Cell Biol.* 111:123–130.

McQuarrie, I. G. 1984. Effect of a conditioning lesion on axonal transport during regeneration: the role of slow transport. *Adv. Neurochem.* 6:185–209.

McQuarrie, I. G., S. T. Brady, and R. J. Lasek. 1986. Diversity in the axonal transport of structural proteins: major differences between optic and spinal axons in the rat. *J. Neurosci.* 6:1593–1605.

McQuarrie, I. G., S. T. Brady, and R. J. Lasek. 1989. Retardation in the slow axonal transport of cytoskeletal elements during maturation and aging. *Neurobiol. of Aging.* 10:359–365.

Mitchison, T., and M. Kirshner. 1988. Cytoskeletal dynamics in nerve growth. *Neuron.* 1:761–772.

Monaco, S., L. Autilio-Gambetti, R. J. Lasek, M. J. Katz, and P. Gambetti. 1989. Experimental increase of neurofilament transport rate: decreases in neurofilament number and in axon diameter. *J. Neuropathol. & Exp. Neurol.* 48:23–32.

Mori, H., M. Komiya, and M. Kurokawa. 1979. Slowly migrating axonal polypeptides. Inequalities in their rate and amount of transport between two branches of bifurcating axons. *J. Cell Biol.* 82:174–184.

Morris, J. R., and R. J. Lasek. 1982. Stable polymers of the axonal cytoskeleton: the axoplasmic ghost. *J. Cell Biol.* 92:192–198.

Morris, J. R., and R. J. Lasek. 1984. Monomer-polymer equilibria in the axon: direct measurement of tubulin and actin as polymer and monomer in axoplasm. *J. Cell Biol.* 98:2064–2076.

Nixon, R. A. 1987. The axonal transport of cytoskeletal proteins: a reappraisal. *In* Axonal Transport. R. S. Smith and M. A. Bisby, editors. A. R. Liss Inc. New York. 175–200.

Nixon, R. A. 1991. Axonal transport of cytoskeletal proteins. *In* The Neuronal Cytoskeleton. R. D. Burgoyne, editor. Wiley-Liss, Inc. New York. 283–307.

Nixon, R. A., and K. B. Logvinenko. 1986. Multiple fates of newly synthesized neurofilament proteins: evidence for a stationary neurofilament network distributed nonuniformly along the axon of retinal ganglion cell neurons. *J. Cell Biol.* 102:647–659.

Oblinger, M. M., and R. J. Lasek. 1988. Axotomy-induced alterations in the synthesis and transport of neurofilaments and microtubules in dorsal root ganglion cells. *J. Neurosci.* 8:1747–1758.

Oblinger, M. M., S. T. Brady, I. G. McQuarrie, and R. J. Lasek. 1987. Cytotypic differences in the protein composition of the axonally transported cytoskeleton in mammalian neurons. *J. Neurosci.* 7:453–462.

Ochs, S. 1982. Axoplasmic transport and its relation to other nerve functions. Wiley-Liss, Inc. New York. 240–264.

O'Farrel, P. H. 1975. High resolution two dimensional electrophoresis of proteins. *J. Biol. Chem.* 250:4007–4021.

Okabe, S., and N. Hirokawa. 1990. Turnover of fluorescently labelled tubulin and actin in the axon. *Nature (Lond.).* 343:479–481.

Paggi, P., and R. J. Lasek. 1987. Axonal transport of cytoskeletal proteins in oculomotor axons and their residence times in the axon terminals. *J. Neurosci.* 7:2397–2411.

Paggi, P., R. J. Lasek, and M. J. Katz. 1989. Slow component B protein kinetics in optic nerve and tract window. *Brain Res.* 504:223–230.

Price, R. L., P. Paggi, R. J. Lasek, and M. J. Katz. 1988. Neurofilaments are spaced randomly in the radial dimension of axons. *J. Neurocytol.* 17:52–62.

Price, R. L., R. J. Lasek, and M. J. Katz. 1990. Internal axonal cytoarchitecture is shaped locally by external compressive forces. *Brain Res.* 530:205–214.

Schliwa, M. 1984. Mechanisms of intracellular transport. *In* Cell and muscle motility. Vol. 5. J. W. Say, editor. Plenum Publishing Corp., New York. 1–82.

Stromska, D., and S. Ochs. 1981. Patterns of slow transport in the sensory nerves. *J. Neurobiol.* 12:441–453.

Tashiro, T., and Y. Komiya. 1989. Stable and dynamic forms of cytoskeletal proteins in slow axonal transport. *J. Neurosci.* 9:760–768.

Watson, D. F., P. N. Hoffman, and J. W. Griffin. 1990. The cold stability of microtubules increases during axonal maturation. *J. Neurosci.* 10:3344–3352.

Willard, M. 1977. The identification of two intra-axonally transported polypeptides resembling myosin in some respects in the rabbit visual system. *J. Cell Biol.* 75:1–11.